HHS Public Access

Author manuscript

Biomaterials. Author manuscript; available in PMC 2020 September 01.

Published in final edited form as:

Biomaterials. 2019 September ; 216: 119245. doi:10.1016/j.biomaterials.2019.119245.

Neurturin-containing laminin matrices support innervated branching epithelium from adult epithelial salispheres

K. H. Vining[1,2,3,8,#], **I. M. A. Lombaert**[1,9,#], **V. N. Patel**[1], **S. E. Kibbey**[1], **S. Pradhan-Bhatt**[4,5,6], **R. L. Witt**[4,5,6,7], **M. P. Hoffman**[1]

[1]Matrix and Morphogenesis Section, National Institute of Dental and Craniofacial Research, NIH, Bethesda, MD, 20842.

[2]Medical Research Scholars Program, Office of Clinical Research Training and Medical Education, Clinical Center, NIH, Bethesda, MD, 20842.

[3]University of Minnesota School of Dentistry, Minneapolis, MN 55455.

[4]Department of Biological Sciences, University of Delaware, Newark, DE, 19716.

[5]Center for Translational Cancer Research, University of Delaware, Newark, DE, 19716.

[6]Helen F. Graham Cancer Center, Christiana Care Health System, Newark, DE, 19713.

[7]Otolaryngology – Head & Neck Surgery, Thomas Jefferson University, Philadelphia, PA, 19107.

[8]Current address: John A. Paulson School of Engineering and Applied Sciences and Wyss Institute for Biologically Inspired Engineering, Harvard University, Cambridge, MA, 02138. U.SA.

[9]Current address: Biointerfaces Institute, University of Michigan, School of Dentistry, North Campus Research Center, 2800 Plymouth Rd, Ann Arbor, MI 48104

Abstract

Cell transplantation of autologous adult biopsies, grown ex vivo as epithelial organoids or expanded as spheroids, are proposed treatments to regenerate damaged branching organs. However, it is not clear whether transplantation of adult organoids or spheroids alone is sufficient to initiate a fetal-like program of branching morphogenesis in which coordinated branching of multiple cell types including nerves, mesenchyme and blood vessels occurs. Yet this is an essential concept for the regeneration of branching organs such as lung, pancreas, and lacrimal and salivary glands. Here, we used factors identified from fetal organogenesis to maintain and expand adult murine and human epithelial salivary gland progenitors in non-adherent spheroid cultures, called salispheres. These factors stimulated critical developmental pathways, and increased expression of

Corresponding author: M.P. Hoffman, National Institute of Dental and Craniofacial Research, NIH, Bethesda, MD 20892, T: 301-496-1660 .

[#]Co-first authors

Author's contributions:

K.H. Vining: Experimental analysis and assembly of data, writing manuscript

I.M.A. Lombaert: Study design, experimental analysis and assembly of data, writing manuscript

S.E. Kibbey: Experimental analysis and assembly of data

V.N. Patel: Experimental analysis and assembly of data

S. Pradhan-Bhatt: Provided human biopsy, experimental planning

R.L. Witt: Obtained human biopsy, experimental planning

M.P. Hoffman: Study design, analysis and assembly of data, writing manuscript

epithelial progenitor markers such as Keratin5, Keratin14, FGFR2b and KIT. Moreover, physical recombination of adult salispheres in a laminin-111 extracellular matrix with fetal salivary mesenchyme, containing endothelial and neuronal cells, only induced branching morphogenesis when neurturin, a neurotrophic factor, was added to the matrix. Neurturin was essential to improve neuronal survival, axon outgrowth, innervation of the salispheres, and resulted in the formation of branching structures with a proximal-distal axis that mimicked fetal branching morphogenesis, thus recapitulating organogenesis. Epithelial progenitors were also maintained, and developmental differentiation programs were initiated, showing that the fetal microenvironment provides a template for adult epithelial progenitors to initiate branching and differentiation. Further delineation of secreted and physical cues from the fetal niche will be useful to develop novel regenerative therapies that instruct adult salispheres to resume a developmental-like program in vitro and to regenerate branching organs in vivo.

Keywords

regenerative medicine; bioengineering; branching morphogenesis; adult epithelial progenitors; fetal microenvironment; salivary gland; ex vivo expansion

INTRODUCTION

The goal to regenerate organs with branched structures has resulted in approaches using stem/progenitor cells, scaffolds, and specific regulatory factors to provide a microenvironment that mimics organogenesis. Recently, progress has been made in culturing somatic tissues such as liver, lung, and kidneys (reviewed in [1]). However, a major barrier is our ability to engineer and/or direct adult tissue-derived stem/progenitors to form multi-cell-type 3D branched structures, recapitulating in vivo organogenesis. This is confounded by the lack of sufficient tissue-specific adult epithelial stem/progenitor cells, termed progenitors hereafter, obtained from small patient biopsies, and the problem of maintaining and expanding them ex vivo.

To achieve functional branching organs, the correct spatial organization of the epithelial progenitors within their organ-specific microenvironment and innervation of the epithelial tissue are essential. One approach to culture adult epithelial progenitors involves dissociating tissues and placing the cells in floating spheroid culture, where tissue-specific epithelial progenitors proliferate, are maintained and/or expanded with specific media conditions (reviewed in [2]). Floating spheroids are distinct from organoids in that the cells are not embedded in an extracellular matrix (ECM), and rely on cell-cell adhesion and their own matrix production. Inducing organ-like structures in this floating cellular context is challenging, and thus spheroids from pancreas [3], prostate [4], intestine [5] and salivary glands [6] have been embedded in ECM, such as Matrigel, with specific growth factors to form organoids. Budding organ-like structures can also be produced from induced pluripotent stem cells [7–9], embryonic stem cells [10], or from single salivary, intestinal, lung, and brain cells [1, 11]. These “mini-organs” are easily replicated, making them ideal for drug testing and in vitro analysis. However, the structures are limited in size and lack

interactions with other cells types such as nerves and blood vessels and do not undergo complex branching morphogenesis, characteristic of developing branching organs.

Another challenge with spheroids and organoids is the in vitro maintenance and expansion of progenitors without differentiation. Self-renewal of epithelial progenitors improved when tissue-specific mesenchymal cells and ECMs were used, as opposed to generic fibroblasts or ECM's [12]. While the inclusion of mesenchymal or endothelial cells enhanced lung and liver organoid growth and differentiation [13–17], their sole presence did not fully induce in vivo-like branching. Importantly, the developmental stage of the niche appeared critical for optimal progenitor expansion. ECM produced by fetal compared to adult mesenchymal cells, offered superior long-term adult mesenchymal progenitor expansion and maintained their differentiation potential [12, 18]. This suggests that the physical and/or non-physical properties of tissue-specific fetal niches may improve adult progenitor expansion and differentiation in vitro.

With respect to the fetal niche, we previously found that nerves and mesenchymal cells provide critical input for epithelial progenitor maintenance during submandibular gland (SMG) branching morphogenesis [19] [20]. The neurons maintain and expand keratin 5 (K5)-expressing progenitors in acetylcholine and HBEGF-dependent pathways, while the mesenchyme produces stem cell factor (SCF) and FGF10, ligands that maintain and expand a second important pool of KIT+FGFR2b+ fetal epithelial progenitors [20]. These KIT +FGFR2b+ progenitors produce the neurotrophic factor neurturin (NRTN) [20], which increases neuronal survival and organ innervation [21, 22]. In contrast, blocking the receptor for NRTN, or genetically deleting NRTN or its receptor, reduces SMG innervation [21, 23, 24]. The nerves in turn produce vasoactive intestinal peptide (VIP) to regulate tubulogenesis and lumen formation of the developing epithelial K5+ ducts [25], which results in enhanced branching morphogenesis. Considering that bidirectional epithelial-neuronal communication is essential for organogenesis, we hypothesized innervation of adult epithelial progenitors may be critical to maintain and expand progenitors to initiate branching morphogenesis in vitro.

Here, we use factors produced by the fetal microenvironment to maintain and expand adult salivary epithelial progenitors in the floating spheroid culture (termed salispheres). Furthermore, adult salispheres recombined in a laminin-111 ECM gel with a fetal mesenchymal microenvironment, which included neurons, required the addition of recombinant neurturin (NRTN) to the ECM to promote epithelial innervation and branching morphogenesis. These findings may improve regenerative approaches using adult epithelial progenitors that require the instructive capabilities of nerves within a complex microenvironment. Neurotrophic support enhanced innervation to induce epithelial branching morphogenesis with the rearrangement of cell types resembling in vivo organogenesis.

MATERIALS AND METHODS

Salisphere culture

Submandibular glands from adult mice (ICR and K5-venus strains) were dissociated into single cells and plated in basal media (BM; DMEM-F12, 1% glutamax, 10 μg/mL insulin (or ITS, 1x), 1% N2, 1 μM dexamethasone, 20 ng/mL FGF2, and 20 ng/mL EGF) at 37°C (5% CO_2, 95% air atmosphere), as described previously [26]. All animal experiments were approved by the Animal Care and Use Committee at NIDCR, NIH. The supplemented media (SM) had additional FGF7 or FGF10 (100 ng/mL, R&D Systems, MN), recombinant mouse stem cell factor (SCF, 100 ng/mL, R&D Systems, MN), the cholinergic-agonist carbachol (Cch, 10 nM, C4382, Sigma), and a ROCK-inhibitor (RI, 5 μM Y27632, Sigma). An EGFR-inhibitor (PD, 10 nM, PD168393, Calbiochem EMD Biosciences) was added (SM+PD). After three days of culture salispheres were analyzed for their size and number. To count the number, salispheres were diluted in PBS (1:30) and counted using a 10x objective. The diameter was measured from 40x images taken with the EVOS-microscope. The diameter and count were combined to give a morphometric-index in arbitrary-units (AU) by multiplying ½ the diameter squared by the count, $((0.5*\text{diameter})^2)*\text{count}$.

qPCR

Gene expression of progenitor cell-type and signaling-pathway markers were measured by qPCR at day zero (D0), three days (D3) and ten days (D10) to track changes in progenitor cell maintenance and expansion in culture. Other genes relevant for SMG development were screened on D10 salispheres. Primers were designed using Beacon Designer software. DNase-free RNA was isolated from salisphere cell lysates and prepared using an RNAqueous-Micro kit and DNase removal reagent (Ambion, Inc. Austin, TX). cDNA (0.5–1 ng) was generated and analyzed by qPCR as previously published [27]. Melt curve analysis was used to verify the generation of a single amplicon. Expression levels were normalized by the delta-delta Ct method to both the housekeeping-gene *Rsp29* and the experimental control group [19].

Immunostaining

Salispheres were fixed in 1–4% PFA or ice-cold acetone-methanol (1:1) after being embedded in a drop of laminin-111 gel (4 mg/ml, Trevigen, MD) on track-etched polycarbonate filters (13 mm, 0.1 μm pore). Samples were blocked for 90 minutes with 10% donkey serum (Jackson Laboratories, ME), 1% BSA, and MOM IgG blocking-reagent (Vector Laboratories, CA) in 0.1% PBS-Tween-20, and incubated with primary-antibodies overnight at 4°C, including rat-anti-Kit (1:100, R&D Systems, MN), rabbit-anti-Keratin-5 (1:2000, Covance Research, NJ), rat-anti-Keratin-19 (1:300, Developmental Biology Hybridoma Bank, University of Iowa)), rabbit-Aqp5 (1:200, Alomone Labs, Israel), mouse-anti-SMA (1:200, Sigma Aldrich, MO), mouse-anti-Ki67 (BD Biosciences), rabbit-anti-Keratin-14 (1:2000, Covance Research, NJ) and rabbit-anti-E-cadherin (1:100,Cell Signaling Technology, MA). Nuclei were stained with Hoechst (1:2000), antibodies were visualized with Cy3- and Cy5-conjugated secondary-Fab fragment antibodies, and samples were imaged with confocal laser-scanning microscopy (CLSM, Zeiss 710 LSM microscopy,

Zeiss, NY). K5-venus+ salispheres were also imaged by EVOS fluorescent-imaging and confocal-microscopy.

Western blot analysis

Salispheres were lysed for protein after 10 days of culture in RIPA Buffer (50mM Tris-HCl pH 7.4, 15 0mM NaCl, 0.1% SDS, 0.5% Na deoxycholate and 1% NP40) and protein concentrations were determined using a BCA standard assay (Pierce, Rockford, IL). Invitrogen 4–12% NuPAGE Bis-Tris Mini Gels were used for electrophoresis of 30–40 ug of protein per lane in reduced conditions, following manufacturer's instructions (Life Technologies, Carlsbad, CA). Proteins were then transferred to PDVF membranes using Invitrogen iBlot Dry Blotting System (Life Technologies, Carlsbad, CA). After transfer, blots were blocked with 5% dehydrated milk in 0.1% TBS-Tween for 1 hour at room temperature. Blots were then incubated in each primary antibody for 1 hour at room temperature or at 4°C overnight. Prior to and following 1 hour secondary incubation (IgG with HRP) at room temperature, blots were washed three times for five minutes, two times for thirty minutes, and three times for five minutes again with 0.1% TBS-Tween. SuperSignal West Dura Chemiluminescent Extended Duration Substrate was used to expose blots (Pierce, Rockford, IL). All Western blots were analyzed using NIH ImageJ software and normalized to Gapdh (Research Diagnostics Inc., Flanders, NJ). The following antibodies were used for western blot analysis: Keratin 5 (Covance, No. PRB-160P) 1:10,000 rabbit, c-Kit (Research Diagnostics, Inc., No. MAB1356) 1:1,000 rat, Smooth Muscle Actin (Sigma Aldrich, No. A 2547) 1:1,000 mouse (monoclonal anti-alpha smooth muscle actin clone 1A4) and GAPDH (Research Diagnostics, Inc., No. RDI-TRK564–6C5) 1:10,000 mouse.

Fluorescence-activated cell sorting

SMGs were prepared for FACS analysis as described [19] with the following modification. Analysis of KIT, FGFR2b, K14, and K5, was previously described (Lomabert et al., 2013), and antibodies labeled with fluorochromes using Dylight (ThermoScientific, NC) or LYNX (AbD Serotec, NC) conjugation kits, according to the manufacturer's instructions. Fluorescence levels were analyzed using FlowJo (Tree Star).

Human salispheres

Human submandibular specimens were procured by Dr. Robert Witt, Newark, DE, from patients undergoing head and neck surgery as previously described [28]. An exemption from the Office of Human Subjects Research at the National Institutes of Health was obtained as no patient identifiers were provided and the specimens were not coded. Salispheres were prepared using the same protocol for mouse salisphere isolation and culture, with 6–8 iterations of enzyme treatment to obtain cell suspension.

Ex vivo recombination

Salispheres from adult female ICR, membrane-Tomato mouse SMGs and human SMG biopsies were cultured in SM for seven to ten days. Salispheres were centrifuged and rinsed in FACs tubes with HBSS/1% BSA. We previously completed dose-response analysis to

determine the NRTN concentration to use with SMG culture and ganglia culture (see Methods in [21]). A solution of 1 ng/μL NRTN + laminin-111 (Cultrex 3D Culture Matrix Laminin 1, 3 mg/ml, Trevigen, MD) was prepared by combining 1 μL of 25 μg/mL NRTN with 24 μL of 50% laminin-111 in cold PBS. Salispheres were pelleted and then a 0.5 uL aliquot of pelleted spheres was mixed in a 0.5 μL drop of the 50% laminin/NRTN on a Sterlitech filter (0.1 μm, PC filter #177601) to achieve a final NRTN concentration of 0.5 ng/μL in the hydrogel. The plates containing the filters were incubated at 37°C for 5 minutes to polymerize the laminin-111. E13 SMGs were harvested from ICR mice and digested with lipase and dispase as previously described. Each E13 SMG organ contains approximately 35,000 cells total, which contain ~27,000 mesenchyme cells and ~700 neuronal cells. We combined 3–4 mesenchymes, which have ~1 PSG ganglia/mesenchyme, to each drop of laminin-111 and salispheres. Controls for the recombination experiments included - intact E13 SMGs cultured for 4 days, embryonic E13 epithelium recombined with endogenous mesenchyme, and salispheres cultured in laminin-111 gel without recombination. Recombination assays were cultured on filters at 37°C for four days with 200 μL of DMEM/F12/P/S media with 150 μg/mL Vitamin C and 50 μg/ml transferrin. The media was replaced every 24 hours. These assays were very consistent with salispheres from multiple preparations undergoing similar levels of branching in all experiments. Branching was quantified by Sholl analysis. Briefly, images were imported in FIJI background subtracted, median filtered, thresholded (Otsu), skeletonized by plugin “Skeletonize 2D/3D”, and pruned to match image [29]. Branching area was measured by the polygon tool and Sholl analysis was performed to measure N (sum of intersections) and to fit a Sholl analysis index for the degree of branching (Schoenen Ramification Index obtained from fitted profile) [30].

Immunostaining of recombined salispheres

The recombination assays were fixed and permeabilized as described above. Then blocked overnight at 4°C in 10% DS, 1% BSA, 1.8% IgG MOM and 0.1% PBST. Primary antibodies were incubated overnight at 4°C in 16% MOM and 0.1% PBST: Pna-Rhodamine (1:75), rabbit anti-K5 (1:2000), mouse anti-Tubb3 (1:200), rabbit anti-Ecadherin (1:100), rat anti-perlecan (1:100). Primary antibodies for human-mouse recombination incubated overnight at 4°C in 16% MOM and 0.1% PBST: mouse anti-Ki67 (1:100), goat anti-Kit (1:100), mouse anti-human nuclear antigen (1:100, Millipore), rabbit anti-Ecadherin (1:100), mouse anti-Tubb3 (1:200), rat anti-integrinβ1 (1:100, Gift of Dr. K.M. Yamada) and rabbit anti-K5 (1:2000). Secondary antibodies incubated for one hour at room temperature in 16% MOM protein and 0.1% PBST: 1:2000 Hoescht, anti-Rabbit cy3 and cy5 (1:200), anti-Mouse cy2 (1:100), anti-goat cy 5 (1:200), and anti-rat cy3 and cy2 (1:200).

Statistical analysis

Error bars represent mean ± standard error of mean (SEM). Experiments were performed with multiple replicates from a minimum of three biologically independent experiments, as specified. Unpaired Student’s t-tests, one-way ANOVA with Dunnett’s or Tukey post-hoc tests, and multiple T-test comparisons with Holm-Sidak method were used to determine statistical-significance of differences, $P<0.05$, between the experimental groups and control (Prism, GraphPad Software). The differences in qPCR data were analyzed by the log(delta-Ct) transform in order to allow us to assume a normal distribution. We used ANOVA with

post-hoc tests and multiple T-test comparisons for analyzing data with multiple genes and conditions to yield much more stringent statistical tests. Error bars show standard error of mean of at least three biological replicates unless otherwise noted.

RESULTS

Signaling pathways important for fetal organogenesis increase the number and size of adult salispheres expressing *Krt5* and *Kit*.

First, we examined whether soluble cues from fetal SMG development could maintain adult SMG progenitors in floating salisphere culture. Adult SMG progenitors were cultured using the standard non-adherent floating salisphere assay, which generates salispheres from adult epithelial cells within 3 days [26, 31, 32]. Salispheres are aggregates of multiple cells, are often not derived from a single cell type, but are enriched for epithelial stem/progenitors. We hypothesized soluble cues from fetal SMG development would help prevent differentiation, and either maintain or increase the cell number of adult progenitors. Fetal KIT+ progenitors require FGFR2b ligands (FGF7 or FGF10 and heparan sulfate), and KIT receptor ligand (SCF) [20], while K5+ progenitor proliferation is induced by the cholinergic agonist carbachol (Cch). On the other hand, ductal K19+ differentiation of K5+ progenitors is blocked by inhibition of the EGF pathway (PD198509) [19]. Therefore, BM was compared to BM supplemented with FGFR2b ligands (FGF10 with heparan sulfate (HS) or FGF7), SCF, and Cch (SM), and/or PD198509 (SM+PD). Our previous works have shown that FGF7 stimulates K5+ progenitor cells and FGF10+HS promotes KIT+ progenitor cells [33, 34]. Rock Inhibitor (RI) was included in both SM and SM+PD to increase survival of any single cell in non-adherent culture [35].

Initially, cells from transgenic K5-venus mice were used to visualize K5+ cells in real time (Fig. 1A). We confirmed that adult K5-venus expression overlapped with endogenous K5 protein (Suppl. Fig. 1A), which is expressed in myoepithelial cells (αSMA+K14+) [36–38] and various duct cells (intercalated KIT+, striated, and excretory K14+ cells) [39–41] (Suppl. Fig. 1B–C). By three days (D3) in culture, more K5-containing spheres were visible in SM+/−PD versus BM. In time (D10), even larger K5-venus expressing spheres were visible in both SM+/−PD (Fig. 1A). The diameter and number of salispheres were measured at D10 to obtain a salisphere index, $Index = R^2N$ (R, radius of sphere; N, number of spheres) (Fig. 1B, graph). Culture in SM+/−PD significantly increased the salisphere index, by increasing sphere diameter and count. Stimulating FGFR2b with either FGF7 (Fig. 1A–E) or FGF10+HS (data not shown) resulted in a similar salisphere index, illustrating both ligands can be applied to increase the sphere index, which suggests a relative increase in epithelial progenitors compared to BM. In preliminary experiments we tested multiple concentrations of each growth factor or used concentrations previously published (data not shown) to obtain an optimal sphere index.

Although not a direct measure of cell number, total RNA content is used as a surrogate measure of cell number when comparing similar cell types, and cultured spheres with SM+/−PD contained significantly more RNA than BM conditions (Fig. 1C). qPCR analysis showed an increased trend of *Krt5* mRNA levels with time in SM+/−PD compared to BM

(Fig. 1D). Interestingly, the expression of the ductal differentiation marker *Krt19* remained unchanged during culture, suggesting the EGFR inhibitor PD was not required to prevent K5+ cell differentiation to K19+ cells in culture. Importantly, SM+/−PD media did significantly increase *Kit* expression with time compared to BM Day 3, although *Kit* expression at Day 10 was not significantly different between the three groups. Western blot analysis of protein expression confirmed that SM+/−PD media generated spheres expressing KIT and increased levels of K5 (Fig. 1E). The level of KIT protein expression at Day 10 was not different between the three groups, which was consistent with *Kit* gene expression at Day 10 (Fig. 1D).

Together, these data suggest that spheres containing adult K5+ and KIT+ progenitors were enhanced when supplemented with factors from the organ-specific fetal microenvironment.

Multiple epithelial cell types expressing progenitor and myoepithelial markers are present in SM-cultured salispheres at D10.

Immunostaining and confocal imaging of murine K5-venus salispheres at D10 in BM conditions confirmed that they contain multiple cell types expressing K5 and KIT (Fig. 2A). However, salispheres cultured in SM [FGF7] contained more epithelial (ECAD, E-cadherin) cells expressing K5 and/or KIT (Fig. 2A), compared to those cultured in BM. Interestingly, various KIT/K5 subpopulations were observed in SM culture; KIT+K5+ (Fig. 2A, dotted arrows), KIT+K5- (Fig. 2A, arrows), and KIT-K5+ (Fig. 2A, arrowheads) cells. Similarly, myoepithelial cells expressing K5, K14 and αSMA (Fig. 2B–C, arrows) as well as basal ductal K5/14+ cells (Fig. 2B–C, arrowheads) and differentiated K19+ cells (Fig. 2C, dotted arrows) were observed. These data suggest that SM maintains the presence of myoepithelial cells, various KIT+ progenitors, basal and differentiated duct cells in culture.

Quantification by FACS analysis (Fig. 2D) confirmed a ~ 3-fold increase in the number of K5-venus expressing cells (21±4% vs. 65±7%) in D10 SM [FGF7 or FGF10+HS] compared to BM. The fraction of KIT+ cells was increased 3-fold (7±2% vs. 19±2%) in SM [FGF10+HS] compared to BM, as well as a trend of increasing FGFR2b+ cells (7±2% vs. 11±3%). The fraction of K14+ cells was increased in SM [FGF7] compared to BM. These data suggest that salisphere culture with SM [FGF7 or FGF10+HS] promoted an increased number of K5+ cells, and that adult KIT+/FGFR2b+ cells are stimulated in SM [FGF10+HS], which is consistent with our previous reports on fetal KIT+/FGFR2b+ cells [20, 34].

Next, we measured expression of genes related to epithelial KIT/FGFR2b, EGFR signaling and acinar cells by qPCR (Fig. 2E) at D10. The expression of epithelial marker *Cdh1,* and downstream targets of KIT/FGFR2b signaling, *Etv5* and *Ccnd1*, were similar in both D10 BM and SM [FGF7] when compared to BM conditions at D3 (dotted line, time when initial spheres form), suggesting FGFR2b-dependent signaling and proliferation at D10 remained at similar levels as D3 in BM. There was no difference in *Egfr* expression, which is expressed in ducts, or its downstream transcription factor *Egr1*, suggesting that ductal differentiation did not change in SM. Similarly, expression of *Aqp5*, which is expressed on acinar cells and intercalated duct cells proximal to the acini [42], did not significantly change in SM. However, we found a significant reduction of *Amy1* and *Muc10*, markers of

mature secretory acinar cells in SM conditions, suggesting SM reduces terminal acinar differentiation over BM conditions. Lastly, the myoepithelial marker, *Acta2*, was significantly higher in BM or SM versus D3 BM conditions, confirming our previous protein results (Fig. 2B–C) that myoepithelial cells survive and grow during salisphere culture.

Taken together, we conclude that salispheres cultured in SM still maintain multiple epithelial cell types within the spheres, with increased expression of progenitor and myoepithelial cell markers, and reduced markers of terminal acinar differentiation.

SM also maintains human epithelial progenitors and myoepithelial cells in salisphere culture

We next investigated whether the beneficial effects of SM conditions were translated to human salisphere culture. Using cells from primary human salivary gland biopsies, D10 spheres in SM [FGF7] conditions formed similar to murine salispheres (Suppl. Fig. 2A). Immunostaining showed that D10 SM salispheres contained epithelial (integrin-β1, ITGB1) cells that expressed K5, K14, KIT and/or αSMA (Fig. 3A). This pattern of protein expression was consistent with murine salispheres, in which the spheres contain multiple epithelial cell types. The latter included KIT+ progenitors, which are present in various human ducts and all or not co-express K5 and/or K14 (Suppl. Fig. 2B). FACS analysis of D10 SM [FGF7] spheres confirmed a consistent presence of ~30–60% KIT+, FGFR2b+, K5+ and K14+ cells. Similar to the mouse model, gene expression levels indicated that KIT/FGFR2b signaling remains present during SM culture (D10 versus D3, dotted line). Myoepithelial markers, *KRT14* and *KRT5* were significantly increased together with an increased trend in *ACTA2*. Most strikingly, we also found a decreasing trend in maturing secretory acinar markers (*PIP*, *MUC7*, *PSP*) over time in SM.

Overall, these data indicate that human-derived spheres in SM culture also keep the presence of various human progenitors, and myoepithelial cells, and most importantly reduce terminal differentiation of acinar cells.

Adult murine salispheres only undergo branching morphogenesis in a fetal mesenchymal microenvironment when innervated

An ex vivo fetal recombination model was used to examine whether D10 SM-cultured adult salispheres could undergo branching morphogenesis in a fetal niche. Adult human or mouse salispheres were placed in laminin-111 extracellular matrix hydrogel to recombine with fetal mouse mesenchyme (Mes) containing developing blood vessels, and the parasympathetic ganglia (PSG) from embryonic day 13 (E13) SMGs (Fig. 4A). Based on our previous work showing that NRTN improves PSG survival and axon outgrowth [19, 21, 22], we hypothesized that NRTN could indirectly promote branching morphogenesis of adult SMG salispheres by enhancing neuronal survival and growth. The laminin hydrogel was used to provide matrix adhesive ligands and to physically position the salispheres in close proximity to mesenchyme tissue (Mes) and/or PSG in order to mimic the spatial orientation of developing organ buds (E13 epi+Mes+PSG).

First, human spheres were recombined within the fetal mouse microenvironment (Suppl. Fig. 3A). We used a Human Nuclear Antigen (HNA) antibody to confirm that cells in the

spheres were human-derived. HNA staining was only observed in the human epithelial E-cadherin (ECAD) compartment, confirming the absence of any contaminating mouse-derived epithelial cells. The human cells in recombined spheres did proliferate, based on KI67 protein staining, and expressed either KIT and/or AQP5. The human salispheres in some cases did grow in association with TUBB3+ nerves (arrow, Suppl. Fig. 3A), but branching was not observed.

There was a significant increase in expression of *CDH1* (an epithelial marker), FGFR2b signaling (*ETV4*, *MYC*), *KRT5*, *KRT14*, *ACTA2* (a myoepithelial marker), and markers of ductal differentiation *KRT19* and *EGFR* (Suppl Fig. 3B). However, expression of acinar markers *AQP5*, *AMY1*, *PIP* and *MUC19* were reduced compared to an adult human SMG. This suggested that, as expected, multiple epithelial cell types were enriched in the recombination assay, but that maturing secretory acinar cells did not develop within 4 days of recombination. The human cells mainly remained as large salispheres within the mouse fetal niche and did not undergo branching morphogenesis, even after 4 weeks in culture (not shown). Further, human salispheres did not undergo branching with the addition of human mesenchymal supplements (SM without PD or ROCK inhibitors) when recombined with PSG+NRTN, but rather grew as aggregates of spheres (Suppl. Fig. 3C). Cross-species incompatibility of mouse fetal tissue with adult human cells may have contributed to this result.

In contrast, syngeneic recombination of mouse adult salispheres with the fetal mouse niche did initiate branching morphogenesis of adult salispheres. In a similar assay, we compared salispheres encapsulated in a laminin-111 hydrogel recombined with the PSG-containing mesenchyme (Mes+PSG) +/− NRTN after 4 days (D4) of culture, compared with primary SMG epithelium in laminin recombined (E13) with PSG-containing mesenchyme as a positive control in the assay for branching morphogenesis, and spheres in laminin without recombination as a negative control (Fig. 4A). Remarkably already by D4, increased epithelial morphogenesis was observed with salispheres recombined with fetal mesenchyme, PSG and NRTN (Fig. 4B–C). The spheres branched in a similar manner to control SMG epithelium. Spheres cultured in the laminin-111 hydrogel simply aggregated without branching, as expected. Surprisingly, when salispheres were recombined with mesenchyme and PSG alone they did not undergo branching morphogenesis, as we initially predicted, and although the spheres were enlarged in size, the PSG neurons did not innervate the epithelium. In contrast, when salispheres were recombined with laminin-111 ECM containing NRTN, with mesenchyme and PSG, the spheres self-assembled, were innervated by PSG neurons (TUBB3, green), and initiated branching morphogenesis, as shown by the formation of ductal structures (K19, cyan) and endbuds (ECAD, red) similar to the fetal epithelium (Fig. 4C). Quantification of skeletonized branching patterns by Sholl analysis showed a trend of higher branching density (N/mm^2) and significantly higher degree of branching (Sholl ramification index) of Sph+Mes+PSG+NRTN compared to Sph+Mes+PSG without NRTN (Fig. 4D).

Higher magnification confocal projections confirmed that neurons (TUBB3) sparsely survived when salispheres were recombined with mesenchyme and PSG without NRTN, suggesting that cues to induce innervation are low or absent under these conditions (Fig.

4E). In contrast, innervation was stimulated in recombined salispheres in laminin-111 ECM containing NRTN with mesenchyme and PSG, as well as in fetal epithelial recombinations, suggesting that exogenous NRTN in the ECM, in addition to NRTN produced by fetal epithelium, stimulate neuronal survival and innervation. The receptor for NRTN, GFRα2, is expressed on the PSG not in the epithelium and so the effect of exogenous NRTN on the epithelium is mediated by the nerves not by NRTN stimulating the epithelium directly [19, 22]. K19 staining further illustrated that the salispheres formed ductal structures and reestablished a proximal-distal axis within the tissue (Fig. 4E), thus recapitulating fetal organogenesis. We previously showed that fetal SMG epithelium expresses NRTN [20], which is why the epithelial recombination was used as a positive control in the assay. We confirmed there was increased expression of *Tubb3*, a marker of neurons, as well as *Ret*, a coreceptor for NRTN, in recombined salispheres with NRTN compared to recombination without NRTN (Fig. 4F). There was also a trend of increased expression of *Vacht* and *Vip*, both functional markers of nerves. *Vacht* is a marker of cholinergic activity and VIP was shown to increase epithelial tubulogenesis in SMGs [21].

Immunostaining with peanut agglutinin (PNA+), which binds the epithelial surface and highlights epithelial morphology, showed epithelial branching structures with highly dense innervation (TUBB3+) along the proximal epithelial ducts where K5+ progenitors were maintained (Fig. 5A). The branching structures contained KIT+ progenitors in the distal endbuds, which were proliferating (KI67+) and expressed the water channel AQP5, a marker for intercalated ducts and acinar cells (Fig. 5B). Thus, cells expressing K5, KIT and AQP5 were localized in the branching adult structures in a similar pattern as in fetal epithelium undergoing branching morphogenesis. This suggests that progenitors within spheres rapidly re-organized themselves within the fetal microenvironment to establish tissue polarity in a similar manner observed during fetal organogenesis. Salisphere recombination with laminin-111 ECM containing NRTN+Mes+PSG not only induced a morphogenesis pattern similar to recombined fetal epithelium, but also showed similar rapid growth kinetics over 4 days (Fig. 4B–C). The epithelial buds and encapsulated spheres showed very little organization at D1, but became fully assembled and branched by 4 days. Furthermore, we confirmed that branched epithelial structures were derived from adult salispheres rather than residual fetal epithelium left in the mesenchyme, by recombining adult mouse spheres from membrane-bound Tomato (mT)-expressing mice with mesenchyme from control mice. Confocal sections clearly illustrated ductal and end-bud structures derived from adult salispheres in the embryonic mesenchyme (Suppl. Fig. 4A–B). Fluorescence imaging of K5 epithelium and Tubb3+ nerves further support the dependence on Mes+PSG+NRTN to generate innervated branching epithelial structures (Suppl. Fig. 4C). We hypothesized that the fetal mesenchyme could be replaced by the addition of SM supplements (without ROCK or PD inhibitors). However, salispheres recombined with PSG+NRTN+Suppl formed aggregates without branching morphogenesis, even when cultures were extended to Day 8 (Suppl. Fig. 4D).

We further characterized the epithelial gene expression profile of the D4 recombined adult salispheres +/− NRTN. Interestingly, we did not find significant changes for genes involved in KIT/FGFR2b signaling, ductal differentiation and/or myoepithelial markers (Suppl. Fig 5A). These data suggest all the cell types survive in the recombinations, with or without

NRTN in the ECM. However, this is in striking contrast to the immunostaining that clearly shows the organization and morphogenesis +/− NRTN is different (Fig. 4B–E). In addition, similar to the human salisphere recombinations, we were unable to detect mature secretory acinar markers (*Psp*, *Smgc*) by D4. However, when recombined glands+NRTN were cultured longer (D8), we were able to observe detectable gene expression levels of *Psp* and *Smgc* compared to D4 E13 SMGs, which had also begun to undergo acinar differentiation (Suppl. Fig 5B). In addition, compared to an intact E13 SMG at D4, the recombined adult salispheres +/− NRTN expressed significantly lower levels of *Ccnd1* and *Fgfr2b*, and significantly higher levels of *Krt5* and *Pecam*, as well as an increasing trend of higher *Acta2* and *Egfr* expression (Suppl. Fig. 5C).

Thus, we show that recombined adult spheres in a laminin-111 ECM +NRTN+PSG and a complex mesenchymal microenvironment grow as innervated branching structures with proper alignment of ductal and acinar cells similar to in vivo development.

DISCUSSION

The regeneration of complex branching adult organs will require multiple cell types and factors, including growth support for nerves and blood vessels. A major challenge in regenerative stem cell therapies is providing sufficient cues to support branching morphogenesis of cells expanded in ex vivo culture, which may lose their capacity for morphogenesis. Here we show how neurotrophic growth factor delivery within a laminin-111 ECM hydrogel has the potential to promote morphogenesis of epithelial progenitors by stimulating neuronal growth and interaction with epithelial cells, which is necessary to recapitulate in vivo organogenesis. We used the intrinsic complexity of the fetal mesenchymal microenvironment as a model system to investigate whether we could stimulate fetal-like branching morphogenesis of adult epithelial salispheres. We discovered that branching was enhanced by the addition NRTN. Importantly, the fetal microenvironment contains neuronal cells. However, additional neurotrophic factor delivery was necessary to promote epithelial innervation, and allow adult progenitors to initiate the developmental program of branching morphogenesis. This approach has significant potential to improve therapeutic regeneration of transplanted tissue-specific progenitor populations or develop implantable artificial tissues.

It has been appreciated for a long time that branching morphogenesis of fetal epithelium requires the physical presence of the surrounding mesenchymal niche [43]. More recently the importance of nerves [19] and blood vessels [44, 45] within this niche has been reported. Although secreted growth factors can support epithelial proliferation and morphogenesis in 3D ECM in the absence of nerves and mesenchyme [33, 46], the epithelial cultures do not recapitulate the robust branching morphogenesis that occurs in the endogenous mesenchyme. The addition of recombinant NRTN improves parasympathetic innervation of the epithelium which aligns with its role as a critical neurotrophic factor for salivary gland innervation during development. In fact, genetic deletion in mice of NRTN or its receptor Gfrα2, results in small parasympathetic ganglia and the mice have multiple defects in epithelial function due to reduced innervation of the gastrointestinal and reproductive tracts as well as the lacrimal and salivary glands [23, 24]. It remains to be determined if the

delivery of NRTN along with adult salispheres into an in vivo adult gland will be necessary to improve innervation and regeneration of the transplanted cells in the adult microenvironment.

In our experiments, human salispheres were unable to branch within a murine fetal microenvironment in a similar manner to mouse salispheres, even with the delivery of NRTN and recombinant human growth factors in the media. We conclude that there may be species-specific cues from human nerves necessary to initiate innervation and branching morphogenesis of the human salispheres. Deciphering these differences between species will be important for human tissue regeneration.

Regeneration of adult salivary glands does occur in rodent models of degeneration caused by ductal ligation. After removal of the ligature, histological structures can be observed that resemble fetal branching morphogenesis, within the context of an adult microenvironment [47]. Importantly, the gland only regenerates if the nerve to the gland is intact. In our recombination studies with salispheres, basal K5+ progenitors within the ductal structures remained in close proximity to nerves, similar to fetal organogenesis. In the proximal endbud, basal KIT+ progenitors surrounded the luminal progeny with a distal-proximal axis, again similar to fetal organogenesis. Moreover, a pattern of gene expression occurred in the adult progenitors similar to fetal organ development. Together, these data suggest that innervation causes adult epithelial progenitors to induce fetal-like gene expression and establish cellular architecture which initiates branching morphogenesis.

An important goal for tissue regeneration is to transplant cells that survive, adapt and function when implanted. Intact fetal salivary and lacrimal glands, pancreas, and kidneys were transplanted in adult rodent environments where they survived and initiated organ-specific functions [48–50], suggesting the adult niche can support a fetal organ transplant. Others developed a functional human liver from an iPSC-derived liver organoids with endothelial and mesenchymal stem cells, which integrated within the local environment and the endothelial cells in reconnected with the host circulation within 48 hours [51]. The physical and biological properties of the microvasculature and surrounding ECM are tissue specific and mesenchymal cell-driven condensation of epithelial progenitors, endothelial cells and mesenchymal stem cells are thus also critical for transplantation of organoids [8]. Thus far, orthotopic gland transplantation of mouse embryonic stem cell-derived salivary gland epithelial aggregates developed into structures with mature acinar cells that became innervated by the recipient mice [10]. Interestingly, an additional recombination of the aggregates with fetal E13.5 mesenchyme was not necessary for this maturation. This suggests that major differences may lie between fetal aggregates and adult spheres, as used in our study, which may require the need for additional neuronal cells and/or NRTN.

Yet, our experiments do not directly address whether the fetal niche may have different effects than an adult niche. Stage-specific signals from fetal niches direct differentiation in ES or iPS-derived cells differently [12]. Fetal rather than adult mesenchyme, induced more differentiation of embryonic stem cell-derived dental epithelial cells [52]. Here, we show that secreted signals from the fetal niche that stimulate FGFR2b, KIT and muscarinic signaling, expand adult epithelial progenitors. We previously showed that K5 expressing

progenitors produce multiple secreted Wnt signals to induce innervation of the duct early in organogenesis [45] and others have shown a role for Wnt ligands [11, 53] during regeneration. The specific role of Wnt signaling in our experimental model of innervation and branching morphogenesis remains to be defined. Further, the potential role of other neuronal cell types, such as Schwann cells or their precursors [54], derived from the co-encapsulated parasympathetic ganglion were not explored here, but likely contribute to branching morphogenesis of adult epithelial progenitors.

In summary, we show that adult epithelial progenitors can be maintained and/or expanded in salisphere culture by factors critical for organogenesis. Salispheres embedded in a laminin-111 ECM containing NRTN form a complex branching tissue when combined with a complex fetal microenvironment that includes neuronal cells. The branching morphogenesis resembles fetal organogenesis, with the correct positioning of epithelial progenitors, their progeny, and induction of fetal gene expression. We propose that support of the neuronal niche, will be essential for regenerative approaches that involve innervation of adult progenitors, so they undergo branching morphogenesis and enable functional organ regeneration.

Supplementary Material

Refer to Web version on PubMed Central for supplementary material.

ACKNOWLEDGMENTS

This research was made possible through the National Institutes of Health (NIH) Medical Research Scholars Program, a public-private partnership supported jointly by the NIH and generous contributions to the Foundation for the NIH from the Doris Duke Charitable Foundation, the American Association for Dental Research, the Colgate-Palmolive Company, Elsevier, alumni of student research programs, and other individual supporters via contributions to the Foundation for the National Institutes of Health. (listed at http://www.cc.nih.gov/training/mrsp/index.html). Research was supported by the Intramural Research Program of the National Institute of Dental & Craniofacial Research at the National Institutes of Health as well as the NIDCR Award Number K08DE025292 (KV).

REFERENCES

[1]. Gjorevski N, Ranga A, Lutolf MP, Bioengineering approaches to guide stem cell-based organogenesis, Development 141(9) (2014) 1794–804. [PubMed: 24757002]

[2]. Pastrana E, Silva-Vargas V, Doetsch F, Eyes wide open: a critical review of sphere-formation as an assay for stem cells, Cell Stem Cell 8(5) (2011) 486–98. [PubMed: 21549325]

[3]. Lim SM, Li X, Schiesser J, Holland AM, Elefanty AG, Stanley EG, Micallef SJ, Temporal restriction of pancreatic branching competence during embryogenesis is mirrored in differentiating embryonic stem cells, Stem Cells Dev 21(10) (2012) 1662–74. [PubMed: 22034992]

[4]. Chua CW, Shibata M, Lei M, Toivanen R, Barlow LJ, Bergren SK, Badani KK, McKiernan JM, Benson MC, Hibshoosh H, Shen MM, Single luminal epithelial progenitors can generate prostate organoids in culture, Nat Cell Biol 16(10) (2014) 951–61, 1–4. [PubMed: 25241035]

[5]. Fordham RP, Yui S, Hannan NR, Soendergaard C, Madgwick A, Schweiger PJ, Nielsen OH, Vallier L, Pedersen RA, Nakamura T, Watanabe M, Jensen KB, Transplantation of expanded fetal intestinal progenitors contributes to colon regeneration after injury, Cell Stem Cell 13(6) (2013) 734–44. [PubMed: 24139758]

[6]. Nanduri LS, Lombaert IM, van der Zwaag M, Faber H, Brunsting JF, van Os RP, Coppes RP, Salisphere derived c-Kit+ cell transplantation restores tissue homeostasis in irradiated salivary gland, Radiother Oncol 108(3) (2013) 458–63. [PubMed: 23769181]

[7]. Lancaster MA, Knoblich JA, Organogenesis in a dish: modeling development and disease using organoid technologies, Science 345(6194) (2014) 1247125.

[8]. Takebe T, Enomura M, Yoshizawa E, Kimura M, Koike H, Ueno Y, Matsuzaki T, Yamazaki T, Toyohara T, Osafune K, Nakauchi H, Yoshikawa HY, Taniguchi H, Vascularized and Complex Organ Buds from Diverse Tissues via Mesenchymal Cell-Driven Condensation, Cell Stem Cell 16(5) (2015) 556–65. [PubMed: 25891906]

[9]. Clevers H, Modeling Development and Disease with Organoids, Cell 165(7) (2016) 1586–1597. [PubMed: 27315476]

[10]. Tanaka J, Ogawa M, Hojo H, Kawashima Y, Mabuchi Y, Hata K, Nakamura S, Yasuhara R, Takamatsu K, Irié T, Fukada T, Sakai T, Inoue T, Nishimura R, Ohara O, Saito I, Ohba S, Tsuji T, Mishima K, Generation of orthotopically functional salivary gland from embryonic stem cells, Nature Communications 9(1) (2018) 4216.

[11]. Maimets M, Rocchi C, Bron R, Pringle S, Kuipers J, Giepmans BNG, Vries RGJ, Clevers H, de Haan G, van Os R, Coppes RP, Long-Term In Vitro Expansion of Salivary Gland Stem Cells Driven by Wnt Signals, Stem Cell Rep. 6(1) (2016) 150–162.

[12]. Sneddon JB, Borowiak M, Melton DA, Self-renewal of embryonic-stem-cell-derived progenitors by organ-matched mesenchyme, Nature 491(7426) (2012) 765–8. [PubMed: 23041930]

[13]. Du Y, Han R, Ng S, Ni J, Sun W, Wohland T, Ong SH, Kuleshova L, Yu H, Identification and characterization of a novel prespheroid 3-dimensional hepatocyte monolayer on galactosylated substratum, Tissue Eng 13(7) (2007) 1455–68. [PubMed: 17518743]

[14]. Lazaro CA, Croager EJ, Mitchell C, Campbell JS, Yu C, Foraker J, Rhim JA, Yeoh GC, Fausto N, Establishment, characterization, and long-term maintenance of cultures of human fetal hepatocytes, Hepatology 38(5) (2003) 1095–106. [PubMed: 14578848]

[15]. McQualter JL, Yuen K, Williams B, Bertoncello I, Evidence of an epithelial stem/progenitor cell hierarchy in the adult mouse lung, Proc Natl Acad Sci U S A 107(4) (2010) 1414–9. [PubMed: 20080639]

[16]. Teisanu RM, Chen H, Matsumoto K, McQualter JL, Potts E, Foster WM, Bertoncello I, Stripp BR, Functional analysis of two distinct bronchiolar progenitors during lung injury and repair, Am J Respir Cell Mol Biol 44(6) (2011) 794–803. [PubMed: 20656948]

[17]. Franzdottir SR, Axelsson IT, Arason AJ, Baldursson O, Gudjonsson T, Magnusson MK, Airway branching morphogenesis in three dimensional culture, Respir Res 11 (2010) 162. [PubMed: 21108827]

[18]. Dissanayaka WL, Zhu L, Hargreaves KM, Jin L, Zhang C, Scaffold-free Prevascularized Microtissue Spheroids for Pulp Regeneration, Journal of Dental Research 93(12) (2014) 1296–1303. [PubMed: 25201919]

[19]. Knox SM, Lombaert IMA, Reed X, Vitale-Cross L, Gutkind JS, Hoffman MP, Parasympathetic Innervation Maintains Epithelial Progenitor Cells During Salivary Organogenesis, Science 329(5999) (2010) 1645–1647. [PubMed: 20929848]

[20]. Lombaert IMA, Abrams SR, Li L, Eswarakumar VP, Sethi AJ, Witt RL, Hoffman MP, Combined KIT and FGFR2b Signaling Regulates Epithelial Progenitor Expansion during Organogenesis, Stem Cell Rep. 1(6) (2013) 604–619.

[21]. Knox SM, Lombaert IMA, Haddox CL, Abrams SR, Cotrim A, Wilson AJ, Hoffman MP, Parasympathetic stimulation improves epithelial organ regeneration, Nat Commun 4 (2013) 1494. [PubMed: 23422662]

[22]. Ferreira JNA, Zheng C, Lombaert IMA, Goldsmith CM, Cotrim AP, Symonds JM, Patel VN, Hoffman MP, Neurturin Gene Therapy Protects Parasympathetic Function to Prevent Irradiation-Induced Murine Salivary Gland Hypofunction, Molecular Therapy - Methods & Clinical Development 9 (2018) 172–180. [PubMed: 29560384]

[23]. Rossi J, Luukko K, Poteryaev D, Laurikainen A, Sun YF, Laakso T, Eerikäinen S, Tuominen R, Lakso M, Rauvala H, Arumäe U, Pasternack M, Saarma M, Airaksinen MS, Retarded Growth

and Deficits in the Enteric and Parasympathetic Nervous System in Mice Lacking GFRα2, a Functional Neurturin Receptor, Neuron 22(2) (1999) 243–252. [PubMed: 10069331]

[24]. Heuckeroth RO, Enomoto H, Grider JR, Golden JP, Hanke JA, Jackman A, Molliver DC, Bardgett ME, Snider WD, Johnson EM Jr., Milbrandt J, Gene Targeting Reveals a Critical Role for Neurturin in the Development and Maintenance of Enteric, Sensory, and Parasympathetic Neurons, Neuron 22(2) (1999) 253–263. [PubMed: 10069332]

[25]. Nedvetsky PI, Emmerson E, Finley JK, Ettinger A, Cruz-Pacheco N, Prochazka J, Haddox CL, Northrup E, Hodges C, Mostov KE, Hoffman MP, Knox SM, Parasympathetic innervation regulates tubulogenesis in the developing salivary gland, Dev Cell 30(4) (2014) 449–62. [PubMed: 25158854]

[26]. Lombaert IMA, Brunsting JF, Wierenga PK, Faber H, Stokman MA, Kok T, Visser WH, Kampinga HH, de Haan G, Coppes RP, Rescue of Salivary Gland Function after Stem Cell Transplantation in Irradiated Glands, Plos One 3(4) (2008).

[27]. Patel VN, Likar KM, Zisman-Rozen S, Cowherd SN, Lassiter KS, Sher I, Yates EA, Turnbull JE, Ron D, Hoffman MP, Specific heparan sulfate structures modulate FGF10-mediated submandibular gland epithelial morphogenesis and differentiation, Journal of Biological Chemistry 283(14) (2008) 9308–9317. [PubMed: 18230614]

[28]. Pradhan S, Liu C, Zhang C, Jia X, Farach-Carson MC, Witt RL, Lumen formation in three-dimensional cultures of salivary acinar cells, Otolaryngology - Head and Neck Surgery 142(2) (2010) 191–195. [PubMed: 20115973]

[29]. Stanko JP, Fenton SE, Quantifying Branching Density in Rat Mammary Gland Whole-mounts Using the Sholl Analysis Method, JoVE (125) (2017) e55789.

[30]. Ferreira TA, Blackman AV, Oyrer J, Jayabal S, Chung AJ, Watt AJ, Sjöström PJ, van Meyel DJ, Neuronal morphometry directly from bitmap images, Nat. Methods 11 (2014) 982. [PubMed: 25264773]

[31]. Rugel-Stahl A, Elliott ME, Ovitt CE, Ascl3 marks adult progenitor cells of the mouse salivary gland, Stem Cell Research 8(3) (2012) 379–387. [PubMed: 22370009]

[32]. Chibly AM, Querin L, Harris Z, Limesand KH, Label-Retaining Cells in the Adult Murine Salivary Glands Possess Characteristics of Adult Progenitor Cells, Plos One 9(9) (2014) 12.

[33]. Steinberg Z, Myers C, Heim VM, Lathrop CA, Rebustini IT, Stewart JS, Larsen M, Hoffman MP, FGFR2b signaling regulates ex vivo submandibular gland epithelial cell proliferation and branching morphogenesis, Development 132(6) (2005) 1223–1234. [PubMed: 15716343]

[34]. Patel VN, Lombaert IMA, Cowherd SN, Shworak NW, Xu YM, Liu J, Hoffman MP, Hs3st3-Modified Heparan Sulfate Controls KIT plus Progenitor Expansion by Regulating 3-O-Sulfotransferases, Developmental Cell 29(6) (2014) 662–673. [PubMed: 24960693]

[35]. Watanabe K, Ueno M, Kamiya D, Nishiyama A, Matsumura M, Wataya T, Takahashi JB, Nishikawa S, Nishikawa S, Muguruma K, Sasai Y, A ROCK inhibitor permits survival of dissociated human embryonic stem cells, Nat. Biotechnol. 25(6) (2007) 681–686. [PubMed: 17529971]

[36]. Ogawa Y, Toyosawa S, Ishida T, Ijuhin N, Keratin 14 immunoreactive cells in pleomorphic adenomas and adenoid cystic carcinomas of salivary glands, Virchows Arch 437(1) (2000) 58–68. [PubMed: 10963381]

[37]. Su L, Morgan PR, Harrison DL, Waseem A, Lane EB, Expression of keratin mRNAs and proteins in normal salivary epithelia and pleomorphic adenomas, J Pathol 171(3) (1993) 173–81. [PubMed: 7506306]

[38]. Reis JS, Simpson PT, Martins A, Preto A, Gartner F, Schmitt FC, Distribution of p63, cytokeratins 5/6 and cytokeratin 14 in 51 normal and 400 neoplastic human tissue samples using TARP-4 multi-tumor tissue microarray, Virchows Arch. 443(2) (2003) 122–132. [PubMed: 12884041]

[39]. Yamamoto M, Nakata H, Kumchantuek T, Sakulsak N, Iseki S, Immunohistochemical localization of keratin 5 in the submandibular gland in adult and postnatal developing mice, Histochemistry and Cell Biology 145(3) (2016) 327–339. [PubMed: 26671786]

[40]. Kwak M, Alston N, Ghazizadeh S, Identification of Stem Cells in the Secretory Complex of Salivary Glands, Journal of Dental Research 95(7) (2016) 776–783. [PubMed: 26936214]

[41]. Song E-AC, Min S, Oyelakin A, Smalley K, Bard JE, Liao L, Xu J, Romano R-A, Genetic and scRNA-seq Analysis Reveals Distinct Cell Populations that Contribute to Salivary Gland Development and Maintenance, Scientific Reports 8(1) (2018) 14043. [PubMed: 30232460]

[42]. Larsen HS, Aure MH, Peters SB, Larsen M, Messelt EB, Galtung HK, Localization of AQP5 during development of the mouse submandibular salivary gland, J. Mol. Histol. 42(1) (2011) 71–81. [PubMed: 21203896]

[43]. Grobstein C, INDUCTIVE EPITHELIO-MESENCHYMAL INTERACTION IN CULTURED ORGAN RUDIMENTS OF THE MOUSE, Science 118(3054) (1953) 52–55. [PubMed: 13076182]

[44]. Lammert E, Cleaver O, Melton D, Role of endothelial cells in early pancreas and liver development, Mechanisms of development 120(1) (2003) 59–64. [PubMed: 12490296]

[45]. Kwon HR, Nelson DA, DeSantis KA, Morrissey JM, Larsen M, Endothelial cell regulation of salivary gland epithelial patterning, Development 144(2) (2017) 211–220. [PubMed: 28096213]

[46]. Morita K, Nogawa H, EGF-dependent lobule formation and FGF7-dependent stalk elongation in branching morphogenesis of mouse salivary epithelium in vitro, Dev Dyn 215(2) (1999) 148–54. [PubMed: 10373019]

[47]. Cotroneo E, Proctor GB, Carpenter GH, Regeneration of acinar cells following ligation of rat submandibular gland retraces the embryonic-perinatal pathway of cytodifferentiation, Differentiation 79(2) (2010) 120–30. [PubMed: 20056310]

[48]. Ogawa M, Oshima M, Imamura A, Sekine Y, Ishida K, Yamashita K, Nakajima K, Hirayama M, Tachikawa T, Tsuji T, Functional salivary gland regeneration by transplantation of a bioengineered organ germ, Nat Commun 4 (2013) 2498. [PubMed: 24084982]

[49]. Hammerman MR, Xenotransplantation of embryonic pig kidney or pancreas to replace the function of mature organs, J Transplant 2011 (2011) 501749.

[50]. Hirayama M, Ogawa M, Oshima M, Sekine Y, Ishida K, Yamashita K, Ikeda K, Shimmura S, Kawakita T, Tsubota K, Tsuji T, Functional lacrimal gland regeneration by transplantation of a bioengineered organ germ, Nat Commun 4 (2013) 2497. [PubMed: 24084941]

[51]. Takebe T, Sekine K, Enomura M, Koike H, Kimura M, Ogaeri T, Zhang RR, Ueno Y, Zheng YW, Koike N, Aoyama S, Adachi Y, Taniguchi H, Vascularized and functional human liver from an iPSC-derived organ bud transplant, Nature 499(7459) (2013) 481–4. [PubMed: 23823721]

[52]. Zheng L, Warotayanont R, Stahl J, Kunimatsu R, Klein O, DenBesten PK, Zhang Y, Inductive ability of human developing and differentiated dental mesenchyme, Cells Tissues Organs 198(2) (2013) 99–110. [PubMed: 24192998]

[53]. Knosp WM, Knox SM, Lombaert IMA, Haddox CL, Patel VN, Hoffman MP, Submandibular Parasympathetic Gangliogenesis Requires Sprouty-Dependent Wnt Signals from Epithelial Progenitors, Developmental Cell 32(6) (2015) 667–677. [PubMed: 25805134]

[54]. Espinosa-Medina I, Outin E, Picard CA, Chettouh Z, Dymecki S, Consalez GG, Coppola E, Brunet J-F, Parasympathetic ganglia derive from Schwann cell precursors, Science 345(6192) (2014) 87–90. [PubMed: 24925912]

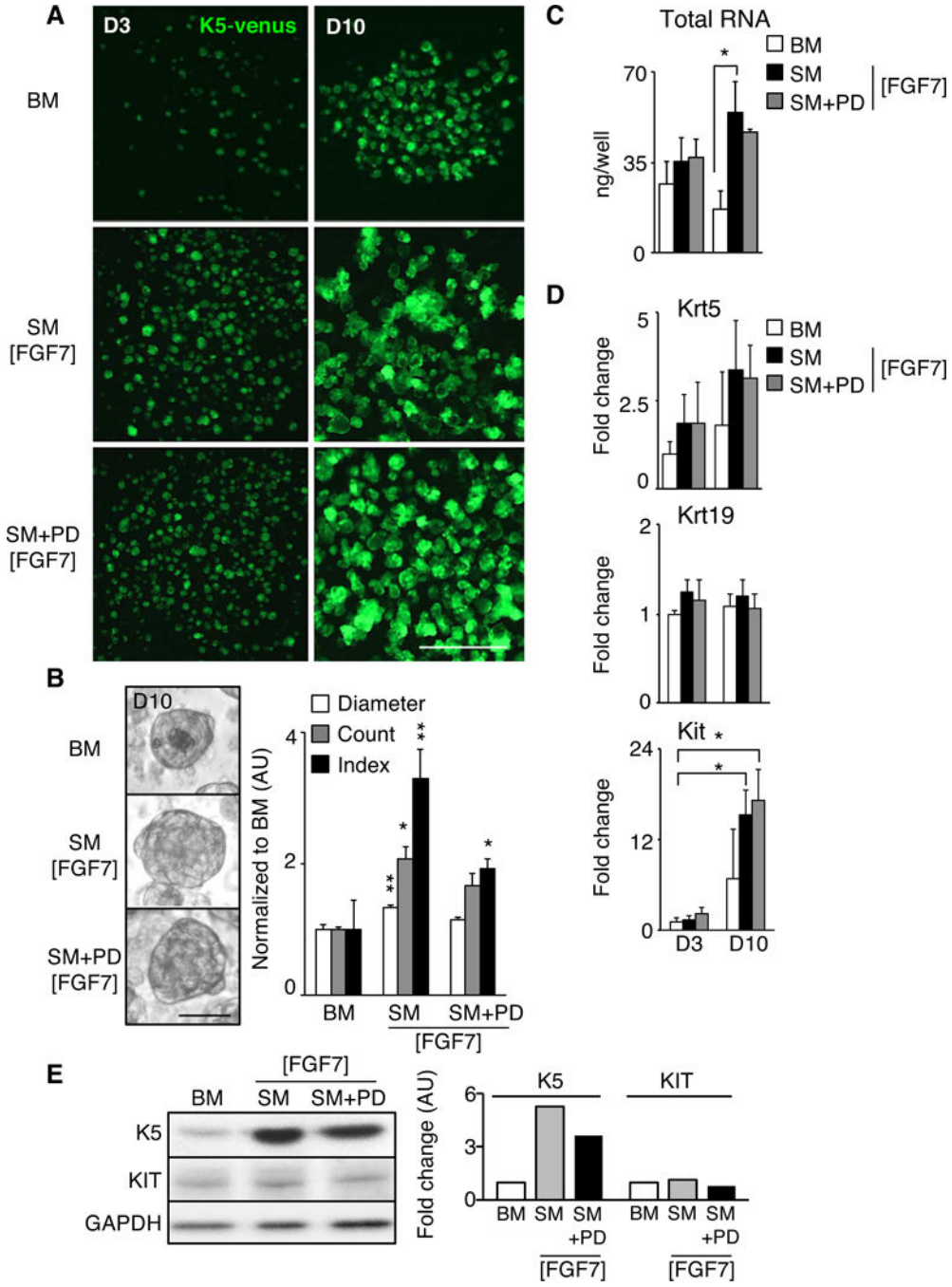

Figure 1. Stimulating signaling pathways important for fetal organogenesis increases the number and size of adult salispheres.

(A) Basal media (BM) was supplemented with FGFR2b ligand FGF7, KIT receptor ligand stem cell factor (SCF), acetylcholine receptor agonist carbachol (Cch), and ROCK inhibitor (RI) to make supplemented media (SM [FGF7]). EGFR inhibitor (PD198509) was added to make SM+PD [FGF7]. Fluorescent images of adult salispheres obtained from K5-venus mice (green) at day three (D3) or D10 in culture. Scale bar, 0.5 mm. **(B)** Bright field pictures of D10 salispheres cultured in BM, SM, or SM+PD. Scale bar, 25 μm. Quantification of

diameter, number (count), and index [Radius^2 x Count] in arbitrary units (AU) of D10 salispheres. *N*=10 biological replicates. Mean±SEM. *, *P*<0.05, **, *P*<0.01, one-way ANOVA with post-Dunnett test compared to BM. **(C-D)** Amount of RNA (ng) obtained from D3 or D10 salispheres in BM, SM and SM+PD, and qPCR analysis of *Krt5*, *Krt19* and *Kit*. Fold changes of gene expression are normalized to *Rsp29* and D3 BM salispheres. *N*=3 biological replicates. Mean±SEM. *, *P*<0.05, one-way ANOVA with post-Dunnett test compared to BM. **(E)** Western blot analyses of salispheres at Day 10. Graph depicts quantification of K5 and KIT normalized to GAPDH expression in arbitrary units (AU). *N*=4 biological replicates, representative blot is shown.

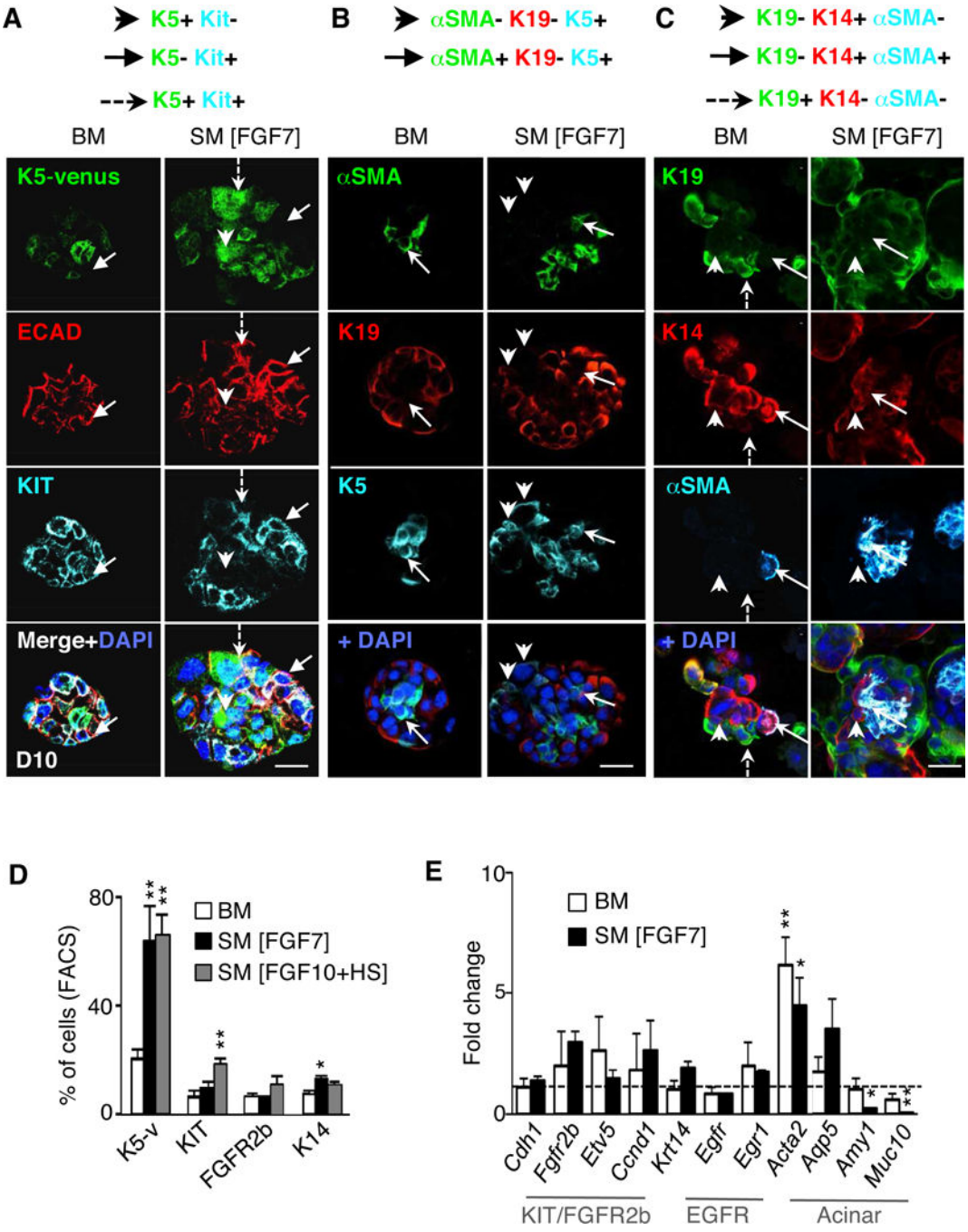

Figure 2. Fetal cues in adult murine salisphere culture (SM) reduce expression of secretory markers and increase cell number of various progenitors.

(A-C) Images of 10 μm confocal sections through D10 salispheres cultured in BM or SM [FGF7], **(A)** showing K5-venus expression with staining for E-cadherin (ECAD, red), KIT (cyan) and/or nuclei (DAPI, blue). Arrowhead, K5+KIT- cells. Arrow, K5-KIT+ cells. Dotted arrow, K5+KIT+ cell. **(B-C)** confocal analysis of αSMA (myoepithelial marker), K19 (ductal marker), endogenous K5, K14, and/or nuclei (DAPI, blue). **(B)** arrows indicate αSMA+K19-K5+ cells, arrowheads indicate αSMA-K19-K5+ cells. **(C)** arrows represent

K19-K14+αSMA+ cell; arrowheads indicate a K19-K14+αSMA- cell. Dotted arrow shows K19+ duct cell. Scale bar, 50 μm. **(D)** FACS analysis (% of total cells) of D10 salispheres cultured in BM, SM [FGF7] or SM [FGF10+HS] media. *N*=3 biological samples. Mean ±SEM. *, $P<0.05$, **, $P<0.01$, one-way ANOVA with post-Dunnett test compared to BM D10. **(E)** Gene expression of D10 salispheres in BM or SM [FGF7], normalized to *Rsp29* and D3 BM salispheres (--). *N*=3 biological samples. Mean±SEM. *, $P<0.05$, **, $P<0.01$, one-way ANOVA with post-Dunnett test.

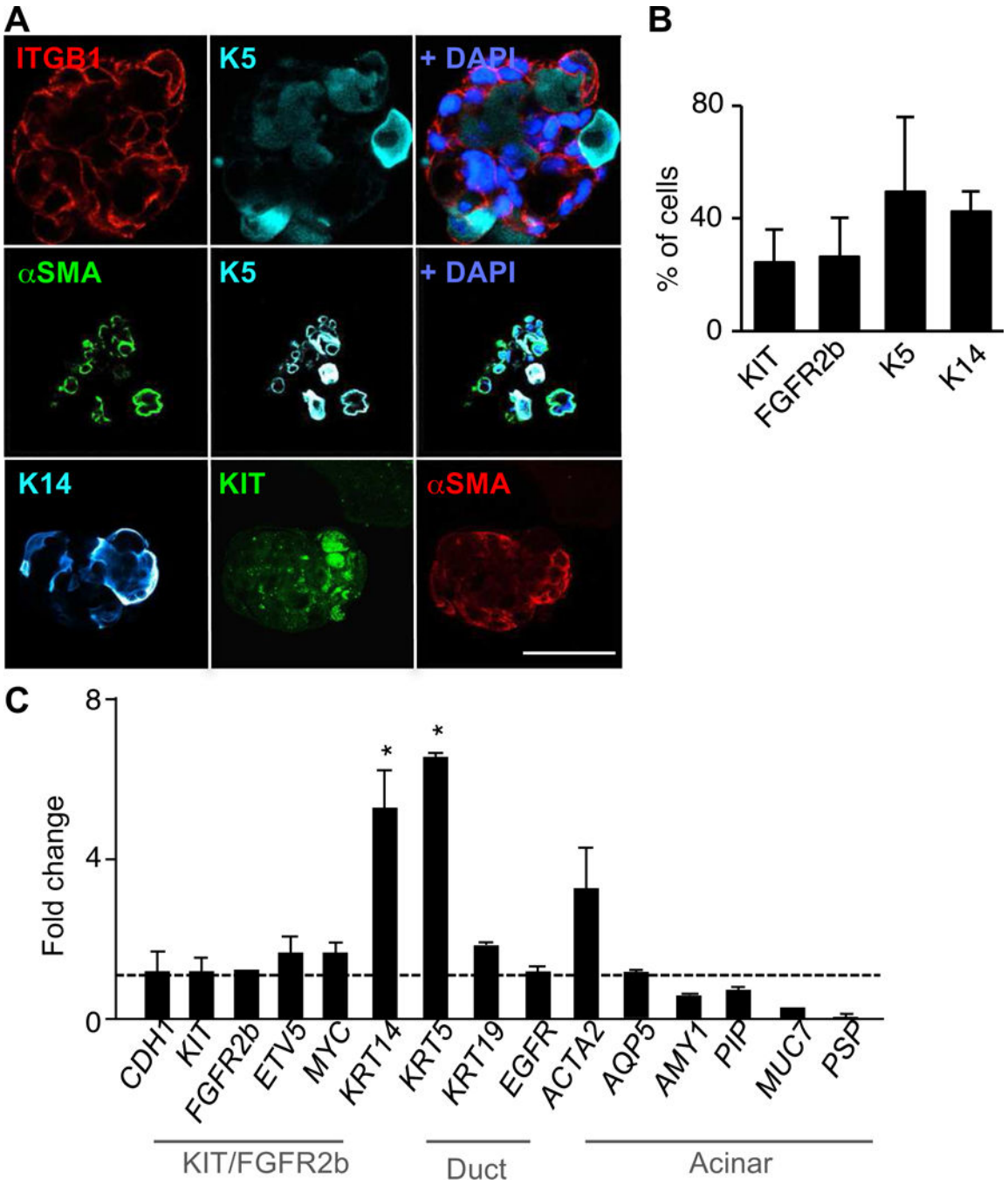

Figure 3. Adult human salispheres in SM contain multiple cell types expressing progenitor and myoepithelial markers.

(A) Confocal 10 μm section of stained D10 salispheres cultured in SM [FGF7] for epithelial marker β1 integrin (ITGB1), K5, αSMA, K14, KIT, and/or nuclei (DAPI, blue). Scale bar, 50 μm. **(B)** FACS analysis (% of cells) of KIT+, FGFR2b+, K5+ and K14+ cells present in D10 SM cultured salispheres. *N*=3 biological samples. Mean±SEM. **(C)** Gene expression of human D10 salispheres cultured in SM [FGF7] and BM, normalized to *RPS29* and SM D3

(dotted line). *, $P<0.05$, one-way ANOVA with post-Dunnett test compared to D3, $N = 4$ biological samples.

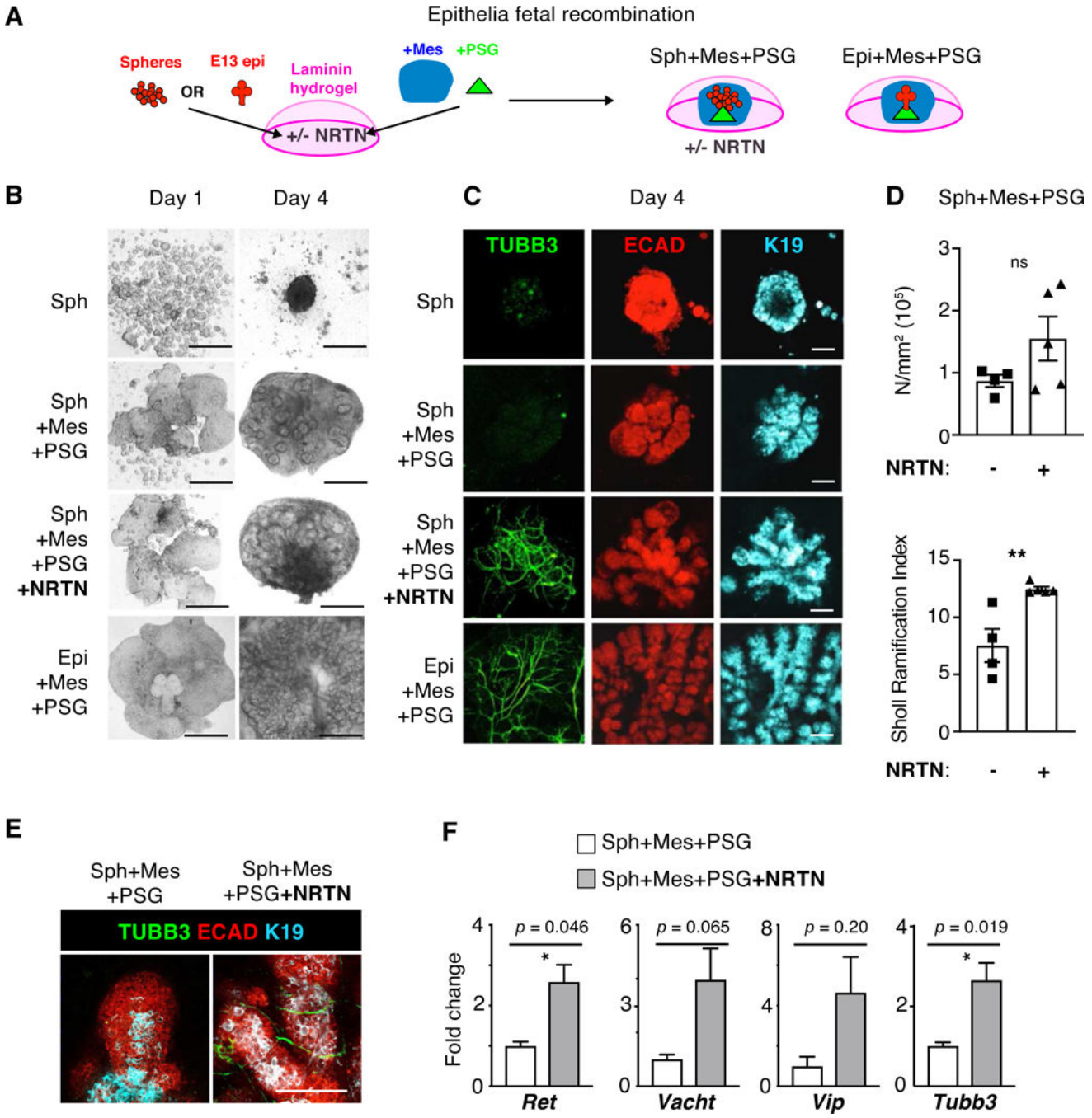

Figure 4. Adult murine salispheres only undergo branching morphogenesis when innervated within a complex fetal microenvironment containing mesenchyme and parasympathetic nerves treated with NRTN.

(A) Cartoon depicting the recombination of adult mouse salispheres that were cultured in SM [FGF7] for 10 days prior to encapsulation in laminin-111 hydrogels. Recombination conditions include E13 parasympathetic ganglia (PSG), mesenchyme containing blood vessels (Mes), and/or recombinant NRTN. Murine E13 SMG epithelia were recombined as a positive control. **(B)** Phase images at days 1 and 4 after recombination. Scale bar, 0.5 mm. **(C)** Confocal 10μm sections of D4 recombined assays of (A), following staining for nerves

(TUBB3, green), epithelia (ECAD – red), ducts (K19 - cyan) and/or nuclei (DAPI, blue). Scale bar, 100 μm. **(D)** Branching density (N/mm^2) and index for degree of branching (Sholl Ramification Index) from Sholl Analysis [29] of D4 recombinations +/− NRTN. *, unpaired two-tailed *t*-test, $P<0.05$. **(E)** Magnified confocal 10μm sections showing D4 recombinations +/− NRTN stained for nerves (TUBB3, green) and epithelial ducts (ECAD - red, K19 - cyan). Scale bar, 100 μm. **(F)** Fold changes of gene expression of neuronal markers in D4 recombined mouse salispheres with or without NRTN, normalized to housekeeping gene *Rps29* and Spheres+Mes+PSG. $N=4$ biological samples. Mean±SEM. *, unpaired two-tailed *t*-test, $P<0.05$.

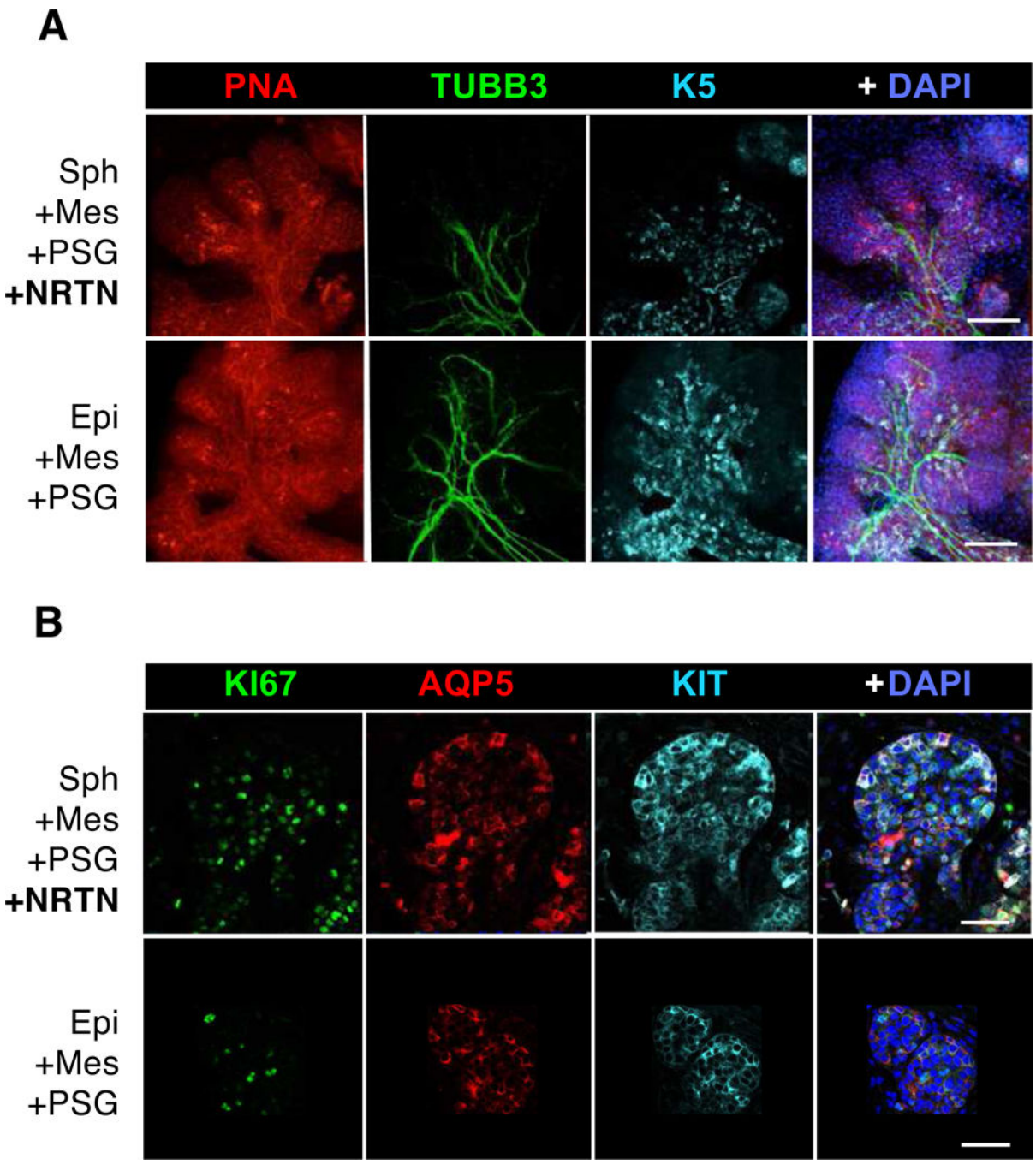

Figure 5. Innervated salisphere-derived branching epithelial structures resemble an ex vivo fetal gland.

D4 recombined mouse adult salispheres **(A)** and fetal epithelium **(B)** in laminin hydrogels with Mes, PSG and NRTN were stained for Peanut Agglutinin (PNA, red) to outline the epithelia, TUBB3 (green) for nerves, K5 (cyan), KIT (cyan), AQP5 (red), KI67 (green) for proliferation and/or DAPI (blue) for nuclei. Confocal images of 10μm sections. Scale bars, 100 μm **(A)** and 50 μm **(B)**.